https://doi.org/10.46813/2025-157-157

NUMERICAL STUDY OF FORMATION OF NEGATIVE STREAMER OF PULSE HIGH-VOLTAGE DISCHARGE IN AIR BUBBLE IN WATER

M.I. Boiko[1], A.V. Makogon[2]
[1]National Technical University "Kharkiv Polytechnic Institute", Kharkiv, Ukraine;
[2]Institute of Electrophysics and Radiation Technologies NAS of Ukraine, Kharkiv, Ukraine
E-mail: qnaboyg@gmail.com, artemmak1991@gmail.com

A mathematical model of the formation of a negative streamer in a pulsed high-voltage discharge in an air bubble in water is proposed. Numerical calculations demonstrate the spatiotemporal development of the streamer within the air bubble, the propagation of the streamer wave toward the «gas (plasma) – water» boundary, the spreading of the discharge along the water surface, and the formation of the most ionized submillimeter region with an electron concentration of ~$7.2 \cdot 10^{16}$ cm^{-3} directly at the tip. In contrast, the average electron concentration in the streamer channel is ~$3 \cdot 10^{15}$ cm^{-3}.

PACS: 52.65.-y, 52.80.-s

INTRODUCTION

The transient nature of discharge processes during water treatment [1, 2] greatly complicates the full understanding of their dynamics. A number of studies have shown that these processes are characterized by intense physicochemical transformations occurring over an extremely short timescale and depending on many interrelated factors, such as the gas composition and the type of electrode system [3], pressure [4], the physical properties of the treated liquid [5], and the parameters of the applied voltage. At the same time, the plasma formed under these conditions exhibits unique properties, including the ability to generate high-energy electrons, reactive nitrogen and oxygen species, various radicals, and intense ultraviolet radiation. It is advisable to create such discharges near the water surface or in gas bubbles within it [6, 7]. The combined effect of factors arising during high-voltage nanosecond discharges in gas bubbles in water can potentially ensure effective sterilization, disinfection, and water purification, contributing to decarbonization of the economy by treating wastewater, thanks to high process efficiency and low energy consumption [8]. This lays the foundation for the development of new environmentally friendly and energy-efficient technologies in the context of current challenges.

The primary mechanism behind the formation of a pulsed nanosecond discharge is impact ionization [9], in which electrons accelerated by a strong electric field gain sufficient energy to ionize neutral gas molecules and atoms through collisions, creating an avalanche of charged particles (an electron avalanche). Impact ionization significantly outweighs other types of ionization due to the high velocity of avalanche development, while thermal effects remain minimal, ensuring the formation of non-equilibrium plasma.

During the development of the discharge in the gas bubble, its conductivity increases relative to that of water, and a significant portion of the voltage is thus applied to the water, creating a strong electric field of up to 70 kV/cm [10]. The treated water can be considered both as a dielectric barrier preventing breakdown and short-circuiting of the system, and as a liquid electrode that facilitates the flow of active current between the plasma zone and the metal electrode in the water. In the contact zone between plasma and water, key mechanisms such as pollutant oxidation and the decomposition of organic compounds are realized. The high dielectric strength of water ensures voltage distribution without breakdown, while its liquid structure promotes the transport of reactive species and contributes to the stability of the system's operation.

To date, there is a lack of a comprehensive mathematical model that would reliably describe the influence of variable applied-voltage parameters (amplitude, pulse duration) on the spatiotemporal dynamics of negative streamer formation in a gas bubble in water, as well as the specifics of the interaction of discharge processes in the two-phase «air bubble (plasma) – water» medium.

The aim of this work is to develop a mathematical model of negative streamer formation in a pulsed high-voltage discharge within an air bubble in water, which will enable determining the effect of the applied voltage on the dynamics of plasma-chemical and electrophysical processes in such discharges.

1. NUMERICAL MODEL

The computer model is based on the application of the finite element method for the numerical solution of equations in a Cartesian coordinate system, in accordance with the methodologies detailed by the authors in scientific works [11–13].

The electron density and the average electron energy are calculated by solving a pair of drift-diffusion equations for electron density and average electron energy:

$$\frac{\partial n_e}{\partial t} + \nabla \cdot \boldsymbol{\Gamma_e} = R_e, \quad (1)$$

$$\boldsymbol{\Gamma_e} = [-n_e(\boldsymbol{\mu_e} \cdot \boldsymbol{E}) - (\boldsymbol{D_e} \cdot \nabla n_e)], \quad (2)$$

$$\frac{\partial n_\varepsilon}{\partial t} + \nabla \cdot \boldsymbol{\Gamma_\varepsilon} + \boldsymbol{E} \cdot \boldsymbol{\Gamma_e} = R_\varepsilon, \quad (3)$$

$$\boldsymbol{\Gamma_\varepsilon} = [-n_\varepsilon(\boldsymbol{\mu_\varepsilon} \cdot \boldsymbol{E}) - (\boldsymbol{D_\varepsilon} \cdot \nabla n_\varepsilon)], \quad (4)$$

where R_e – is the electron source (the rate of electron generation; $1/(m^3 \cdot s)$), R_ε – is the energy loss due to

inelastic collisions; $n_\varepsilon = n_e \cdot \varepsilon_c$ (ε_c – is the average electron energy); n_e – is the electron concentration; $\boldsymbol{\mu_e}$ – is the electron mobility; $\boldsymbol{D_e}$ – is the electron diffusion coefficient; $\boldsymbol{D_\varepsilon}$ – is the diffusion coefficient for the average electron energy; $\boldsymbol{E}$ – is the electric field strength; $\boldsymbol{\Gamma_e}$, $\boldsymbol{\Gamma_\varepsilon}$ − are the flux vectors of electron energy and electrons, respectively.

The coefficients for the electron source in the equations above are determined by the chemical composition of the plasma, while the electron energy losses were obtained by summing the energy losses from collisions in all reactions.

The reaction rates r are calculated according to the law of mass action, where the reaction rate coefficients can be computed from cross-sectional data using the following integral:

$$k^f = \gamma \int_0^\infty \varepsilon \cdot \sigma_k(\varepsilon) \cdot f(\varepsilon) d\varepsilon, \quad (5)$$

$$r = k^f \prod_{k=1}^{i} C_k^v, \quad (6)$$

C_k^v – concentrations of species k (v – are the stoichiometric coefficients); $\gamma = (2 \cdot k_v/m_e)^{1/2}$ ($C^{1/2}/kg^{1/2}$); m_e – the mass of an electron (kg); ε – energy (eV); $\sigma_k(\varepsilon)$ – collision cross-section (m^2); $f(\varepsilon)$ – he electron energy distribution function.

The prescribed (given) function for the electron energy distribution is given in the following generalized form:

$$f(\varepsilon) = g\varphi^{-3/2} \cdot \beta_1 \cdot e^{\left(\frac{-\varepsilon \cdot \beta_2}{\varphi}\right)^g}, \quad (7)$$

where $\beta_1 = \Gamma(5/2g)^{3/2} \cdot \Gamma(3/2g)^{-5/2}$; $\beta_2 = \Gamma(5/2g)^1 \Gamma(3/2g)^{-1}$; φ – average electron energy (eV); ε – electron energy (eV); Γ – incomplete gamma function for electrons; g = 1.7.

In a nanosecond nonequilibrium discharge, the electron energy distribution does not correspond to the pure Maxwellian (g = 1) or Druyvesteyn (g = 2) models. Therefore, an intermediate generalized function with the parameter g = 1.7 is proposed, which takes into account the «tail» of high-energy electrons and suppresses the accumulation of very hot electrons.

For non-electron reactions, a multicomponent diffusion equation is solved, where the diffusion model is averaged over the mixture.

The electric field strength is calculated using the following dependence (Poisson's equation):

$$-\nabla(\varepsilon_0 \varepsilon_r \boldsymbol{E}) = \rho, \quad (8)$$

$$\boldsymbol{E} = -\nabla V, \quad (9)$$

where V – the potential; ρ – the charge density; ε_r – the relative dielectric permittivity of the material; ε_0 – the absolute dielectric permittivity of vacuum.

Electron current density and displacement current density were calculated using the following expressions:

$$\boldsymbol{J_e} = -e \cdot (n_e \boldsymbol{\mu_e} \boldsymbol{E} + \boldsymbol{D_e} \cdot \nabla n_e), \quad (10)$$

$$\boldsymbol{J_D} = \frac{\partial \boldsymbol{D}}{\partial t}, \quad (11)$$

where $\boldsymbol{J_e}$ − electron current density; $\boldsymbol{J_D}$ – displacement current; $\boldsymbol{D}$ – electric displacement vector.

In Table, a simplified model of plasma-chemical reactions is presented. In the performed simulation, these reactions are considered at the leading edge of the pulse, and it can be assumed that an approximation to the real processes in the bubble during streamer formation has been achieved. At this stage, the processes of photoionization, thermionic emission, and air humidity are not taken into account.

Plasma-chemical reactions in the gas bubble

Plasma-chemical reactions	Constants – $cm^3\ s^{-1}$, $cm^6\ s^{-1}$ (for three-component reactions)	Energy loss upon collision (activation energy) – eV
1.e + O_2 => e + O_2 (elastic collisions)	*K=f(e)*	–
2. e + O_2 => O + O-	*K=f(e)*	–
3.e + O_2 => e + O_2	*K=f(e)*	0.02, 0.19, 0.38, 0.57, 0.75
4.e+O_2=>e+$O_2(a^1)$	*K=f(e)*	0.98
5. e+$O_2(a^1)$=>e+O_2	*K=f(e)*	-0.98
6. e+O_2=>e+$O_2(b^1)$	*K=f(e)*	1.63
7. e+ $O_2(b^1)$=>e+O_2	*K=f(e)*	-1.63
8. e+O_2=>e+$O_2(A^3)$	*K=f(e)*	4.5
9. e+ $O_2(A^3)$=>e+O_2	*K=f(e)*	-4.5
10. e + O_2 => e + O + $O(^3P)$	*K=f(e)*	6.1
11. e + O_2 => e + O + $O(^1D)$	*K=f(e)*	8.4
12. e + O_2 => e + O + $O(^1S)$	*K=f(e)*	9.97
13. e + O_2 => 2e + O2+ (ionization)	*K=f(e)*	12.06
14. O-+O2+=>O+O+O	$2.6 \cdot 10^{-8} \cdot (300/T)^{0.44}$	–
15. O- + O => O_2 + e	$5 \cdot 10^{-10}$	–
16. e + N_2 => e + N_2 (elastic collisions)	*K=f(e)*	–
17. e + N_2 => e + N_2	*K=f(e)*	0.02, 0.29, 0.59, 0.88, 1.17, 1.76, 2.06, 2.35
18. e+N_2=>e+$N_2(A^3)$	*K=f(e)*	6.17…7.0
19. e+N2=>e+N2(B^3)	*K=f(e)*	7.35…7.8
20. e+N2=>e+N2(W^3)	*K=f(e)*	8.16
21. e+N_2=>e+$N_2(A'^3)$	*K=f(e)*	8.4
22. e+N_2=>e+$N_2(a''^1)$	*K=f(e)*	8.55

23. $e+N_2=>e+N_2(C^3)$	*K=f(e)*	8.89
24. $e+N_2=>e+N_2(E^3)$	*K=f(e)*	11.03
25. $e+N_2=>e+N_2(G^3)$	*K=f(e)*	11.87
26. $e+N_2=>N_2-$	*K=f(e)*	–
27. $e+N_2+N_2=>N_2-+N_2$	$1.41\cdot10^{-37}$	–
28. $e+N_2=>2e+N_2+$(ionization)	*K=f(e)*	15
29. $e+N_2=>2e+N_2+$(ionization)	*K=f(e)*	18.1
30.$e+O2+=>0.9O(^1D)+0.1O(^1S)+O(^3P)$	$1.9\cdot10^{-7}\cdot(300/T_e)^{0.5}$	–
31. $e + N_2+=> N_2$	$5\cdot10^{-8}$	–
32. $N_2- + N_2+=> N_2 + N_2$	$2\cdot10^{-6}$	–
33. $e+O_2+=>O+O$	$1\cdot10^{-7}$	–
K=f(e) – it means that the constant was calculated using the electron distribution function, *T*– gas temperature		

In Table, two-particle reactions involving oxygen and nitrogen atoms and molecules − in both excited and ground states − are presented, which describe the processes in discharges in air at atmospheric pressure. The dependence of collision cross-sections on energy for calculating the rate constants of electron reactions via the electron energy distribution function is taken from the following sources: [9, 14, 15]. In the air plasma model (N_2/O_2), elastic collisions without energy losses (reactions 1, 16) play an important role, as do inelastic excitations of the electron levels of oxygen (4), (6), (8), (9) and nitrogen (18)−(25), where characteristic singlet and triplet states are formed. Ionization (13), (28), (29) generates electron–ion pairs, and O_2 dissociation (10)−(12) produces oxygen atoms O (^{3}P, ^{1}D, ^{1}S), which participate in subsequent chemical reactions. At the same time, negative ions O^- (2) and rare channels of N_2^- formation (26) or a three-particle process (27) occur. Recombination reactions (14), (15), (30−33) return the system to neutrality. Multiple collisions (3), (17) between electrons and neutral atoms with electron energy losses also contribute to the electron energy distribution, while high-energy processes dominate in the formation of the streamer channel. Metastable states and ion–ion recombination accelerate the decay of the plasma.

In the presented photo (Fig. 1), nanosecond high-voltage discharges that occur in gas bubbles of air in water are illustrated, obtained using a high-voltage prototype of a continuous-flow technological installation for water disinfection, which is described in detail in the article [16].

The pulse repetition frequency in experiments with such discharges was approximately 2000 pulses/s, the current amplitude reached 100 A, and the voltage amplitude – 30 kV. The pulse duration was about 60 ns with a rise time of 10 ns.

The Fig. 2 shows a graphical model of the reactor with an interelectrode gap corresponding to the gap where the experimental nanosecond discharges in gas bubbles in water were obtained, which was used for the calculations.

Fig. 1. Photo of experimental nanosecond discharges in gas bubbles in water

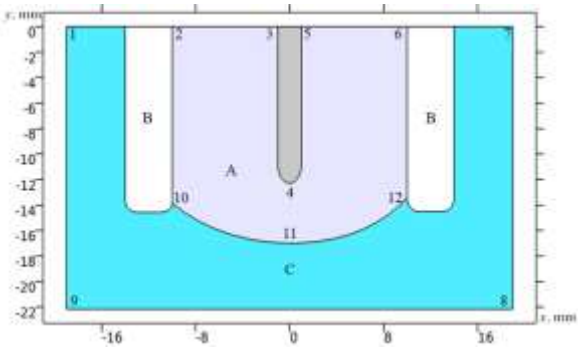

Fig. 2. Reactor model and interelectrode gap

Region A – model gas bubble, where plasma-chemical reactions occur directly – ideal gas, C – water with a dielectric permittivity of 80, B – housing made of a material with a dielectric permittivity of 2.3. The temperature of the gas, water, and housing is T = 300 K, and the pressure is one atmosphere.

For the boundaries 1-2, 6-7 in the figure, a zero-charge condition is specified:

$$-\boldsymbol{n}\cdot\boldsymbol{D}=0. \quad (12)$$

For the boundaries 2-3 and 5-6, insulation conditions are specified that correspond to the inlets or outlets of the background gas. The boundary condition sets the normal component of the electron flux and the electron energy flux to zero:

$$-\boldsymbol{n}\cdot\boldsymbol{\Gamma}_e=0, \quad (13)$$

$$-\boldsymbol{n}\cdot\boldsymbol{\Gamma}_{\boldsymbol{\varepsilon}}=0. \quad (14)$$

For regions C and B, a charge conservation condition is specified that incorporates the charge conservation equation according to Gauss's law for the electric displacement field in a dielectric:

$$\boldsymbol{D} = \varepsilon_0 \varepsilon_r \boldsymbol{E}. \quad (15)$$

The change in the high-voltage electrode potential at the boundary 3-4-5 (tip – width 2 mm, rounding radius 1 mm) as shown in the Fig. 3:

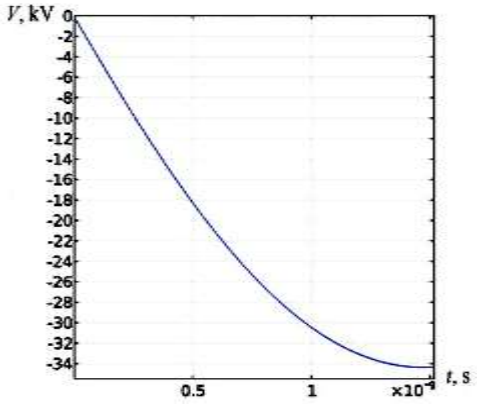

Fig. 3. Change in the potential of the high-voltage electrode

Boundary 1-9-8-7, in turn, is the boundary between the water volume and the low-voltage electrode, i.e., the surface of the low-voltage electrode that is adjacent to the water, with V_0 = 0 V.

For boundaries 2-10, 12-6, 3-4-5, 10-11-12, a wall boundary condition is specified that describes the interaction of the plasma when it comes into contact with surfaces. The resulting equation for the normal component of the electron flux at the wall is given by:

$$\boldsymbol{n} \cdot \boldsymbol{\Gamma}_\mathrm{e} = \left(\frac{1}{2} V_{e,th} \cdot n_e\right), \quad (16)$$

and for the normal component of the electron energy density:

$$\boldsymbol{n} \cdot \boldsymbol{\Gamma}_{\boldsymbol{\varepsilon}} = \left(\frac{5}{6} V_{e,th} \cdot n_\varepsilon\right), \quad (17)$$

$V_{e,th}$ – thermal speed (m/s).
The thermal speed is defined as:

$$V_{e,th} = \sqrt{\frac{8 k_b T_\mathrm{e}}{\pi m_e}}, \quad (18)$$

where k_b – Boltzmann constant; T_e – electron temperature; m_e – electron mass.

At the boundary 10-11-12 (the interface between the gas bubble and water), a surface charge accumulation condition is specified:

$$\frac{d\sigma_s}{dt} = \boldsymbol{n} \cdot \boldsymbol{J_i} + \boldsymbol{n} \cdot \boldsymbol{J_e}, \quad (19)$$

where σ_s – surface charge density (C/m²), $\boldsymbol{J_i}, \boldsymbol{J_e}$ – ion and electron current densities (A/m²), $\boldsymbol{n}$ – unit normal vector to the surface

For the calculation of the ion current on the walls using the method presented in [13], at the boundaries in the gas bubble and at the electrode boundary, surface ion recombination reactions are specified: N_2^- => N_2 , O^- => O, O_2^+ => O_2 , N_2^+ => N_2 , with a sticking coefficient of 1, and it is established that the ion current density is orders of magnitude lower than the displacement current density and the electron current density.

Charge accumulation leads to a discontinuous electric displacement field on the dielectric surfaces:

$$-\boldsymbol{n}(\boldsymbol{D_1} - \boldsymbol{D_2}) = \sigma_s, \quad (20)$$

where $\boldsymbol{D_1}$, $\boldsymbol{D_2}$ – the electric displacement vectors on the inner and outer sides of the dielectric surface (water).

Modeling of the processes in the reactor was performed in a time interval from 0 to 1.5 ns with a time step of 0.001 ns, which ensured the voltage rise to its amplitude value. The computational domain was discretized with a triangular grid with a characteristic element size ranging from 0.019 to 0.23 mm. At the zero moment, the electron concentration n_e = $1 \cdot 10^6$ cm^{-3}, the negative ion concentration n_i (N_2^-, O^-) = $2 \cdot 10^6$ cm^{-3}, the positive ion concentration n_i (N_2^+, O_2^+) = $3 \cdot 10^6$ cm^{-3}, the electron energy ε = 0.1 eV, the initial concentrations of N_2 (75 %) = $1.97 \cdot 10^{19}$ cm^{-3}, the concentration of O_2 (18 %) = $4.73 \cdot 10^{18}$ cm^{-3}, and all other species constitute 7 % of the plasma ≈ $2.63 \cdot 10^{11}$ cm^{-3} for each. The specified initial composition of the gas bubble approximately corresponds to atmospheric air, indicating the initial background before the discharge.

2. CALCULATION RESULTS AND THEIR DISCUSSION

In the Fig. 4, the formation of a negative streamer in an air bubble in water is shown.

At the initial stage (up to 0.8 ns) a zone of enhanced ionization is formed near the tip (a sharp increase in the electron concentration to ~$4.1 \cdot 10^{14}$ cm^{-3}), which triggers a streamer wave that propagates from the tip to the gas – water interface. By 1.28 ns this streamer transforms into a well-conducting channel with subsequent spreading of the discharge up to 4 mm along the dielectric surface (water) in the form of a sliding surface discharge, and when at 1.5 ns the voltage reaches its maximum, the most ionized submillimeter region ($7.2 \cdot 10^{16}$ cm^{-3}) is formed directly near the tip with an average concentration of $3 \cdot 10^{15}$ cm^{-3} of charged micro-particles in the already formed streamer channel in the air bubble between the tip and the water surface. The modeling results of the obtained concentrations are compared with experimental data obtained by other authors for a diffuse nanosecond discharge in a similar «tip – plane» electrode configuration in dry air under high overvoltage [17]. In [17] it was established that most of the volume is occupied by quasi-stationary plasma, where the electron concentration is ~10^{15} cm^{-3} and the average energy is ~3 eV. At the same time, a submillimeter zone with increased ionization is formed near the tip (n_e >10^{17} cm^{-3}, degree of ionization >1 %), which is accompanied by intense emission in a wide spectral range. In contrast to a diffuse discharge, where ionization is uniformly distributed throughout the entire volume, in the case of discharges in an air bubble in water the modeling reveals a localized ionization zone and a sharp increase in the electron concentration at the

streamer front, indicating the dominance of the avalanche-streamer mechanism. At the same time, it is impossible to rule out the possibility of primary ionization mechanisms throughout the entire bubble [18], which may precede the streamer process, especially under conditions of high overvoltage. This may lead to the formation of an initial ionized background that subsequently focuses into a narrow conductive streamer channel.

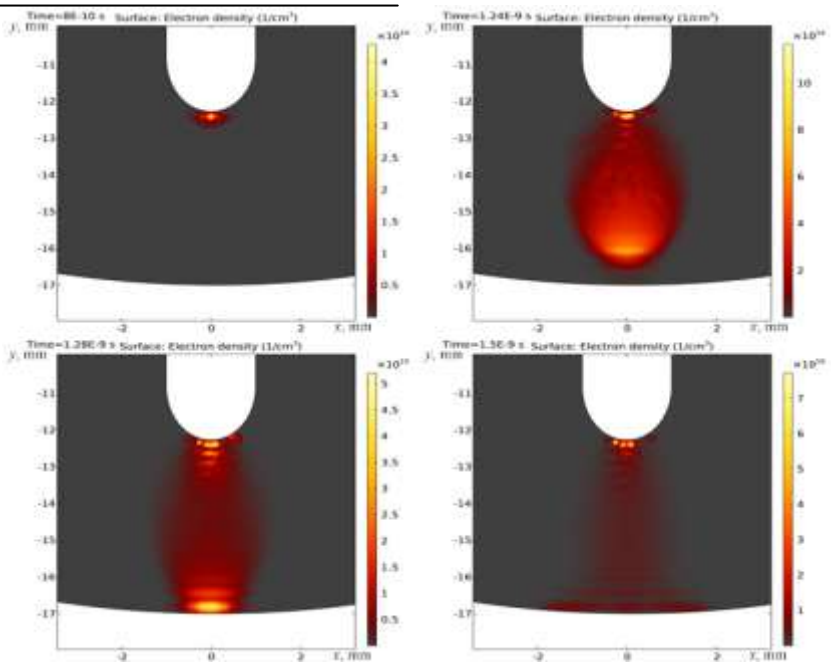

Fig. 4. Formation of negative streamer in an air bubble

CONCLUSIONS

The proposed mathematical model for the formation of a negative streamer in an air bubble in water allows for the effective investigation of key aspects of plasma processes−specifically, it has been demonstrated through calculations that the development of a negative streamer is accompanied by avalanche-like ionization and the formation of a conductive channel. The most intense processes occur in narrow, localized zones, particularly near the electrode tip and the streamer head during its formation.

Further results, covering the analysis of potential distribution, electric field strength, electron temperature distribution, current density, and the concentrations of the main charged and excited species in the air bubble during the formation of the negative streamer, will be presented in subsequent studies.

The use of high-voltage pulsed discharges in gas bubbles for water treatment is an innovative approach that addresses modern environmental challenges, as it enables the concentration of the entire set of active factors directly in the treated water.

ACKNOWLEDGEMENTS

The work of A.V. Makogon is financially supported in part by the scholarship named after Academician NAS of Ukraine B.Ye. Paton for young scientists of the National Academy of Sciences of Ukraine.

REFERENCES

1. Garima Arora et al. Properties and characteristics of the nanosecond discharge developing at the water–air interface: tracking evolution from a diffused streamer to a spark filament // *Plasma Sources Sci. Technol*. 2024, 33, p. 025025; DOI 10.1088/1361-6595/ad257d

2. I.N. Onishchenko, G.V. Taran, O.O. Zamuriev, P.O. Opalev. Study of electrodynamics' characteristics of gas discharge in a needle-plane system with one liquid electrode // *Problems of Atomic Science and Technology*. 2024, № 6, p. 122-126. https://doi.org/10.46813/2024-154-122

3. Bo Jiang et al. Review on electrical discharge plasma technology for wastewater remediation // *Chemical Engineering Journal*. 2014, v. 236, p. 348-368. http://doi.org/10.1016/j.cej.2013.09.090

4. Likai Xiong et al. Numerical simulation analysis of discharge in water under different pressures // *IEEE Transactions on Dielectrics and Electrical Insulation*. 2024, v. 31, issue 5, p. 2461-2468.

5. A. Herrmann, J. Margot, A. Hamdan. Experimental and 2D Fluid Simulation of a Negative Nanosecond Discharge in Air Above a Liquid Surface with Different Dielectric Permittivity and Electrical Conductivity // *Plasma Chem Plasma Process*. 2025. v. 45, p. 191-209. https://doi.org/10.1007/s11090-024-10525-0

6. Z. Chen, Y.E. Krasik, S. Cousens, A.T. Ambujakshan, C. Corr, X.J. Dai. Generation of underwater discharges inside gas bubbles using a 30-needles-to-plate electrode // *J. Appl. Phys.* 2017, v. 122, p. 153303. https://doi.org/10.1063/1.4993497

7. Y. He, S. Uehara, H. Takana, H. Nishiyama. Numerical and Experimental Investigation of Acetic Acid Decomposition by a Nano-Pulse Discharged Bubble in Water // *International Journal of Plasma Environmental Science and Technology*. 2018, v. 12, N 1, p. 30-36.
8. M.I. Boiko, A.V. Makogon. Energy-efficient technology for water disinfection in a flow using pulsed high-voltage discharges // *Problems of Atomic Science and Technology*. 2024, № 6, p. 141-145. https://doi.org/10.46813/2024-154-141
9. Yu. P. Raizer. *Gas Discharge Physics*. Berlin: Springer, 1991, 449 p.
10. M.I. Boiko, A.V. Makogon. Features of distribution of electric field strength and current density in the reactor during treatment of liquid media with high-voltage pulse discharges // *Electrical Engineering and Electromechanics*. 2024, №5, p. 58-63. https://doi.org/10.20998/2074-272X.2024.5.08
11. Zhehao Zhang et al. Simulation of hollow- cathode- nitriding plasma and design of diffusion equipment with DC and RF dual discharge // *Physica Scripta*. 2023, v. 98, N. 2, p. 025610. DOI 10.1088/1402-4896/acb330
12. Yizhuo Zhang, Shengwang Yu, Jie Gao, Yong Ma, Zhiyong He, Hongjun Hei, Ke Zheng. Design and simulation of a novel MPCVD reactor with three- cylinder cavity // *Vacuum*. 2022, v. 200, p. 111055. DOI 10.1016/j.vacuum.2022.111055
13. Navin Kumar Sharma, Shikha Misra, Varun, Udit Narayan Pal. Experimental and simulation analysis of dielectric barrier discharge based pulsed cold atmospheric pressure plasma jet // *Phys. Plasmas*. 2020, v. 27, p. 113502. DOI 10.1063/5.0018901
14. NIST Chemical Kinetics Database [Online]. Available: https://kinetics.nist.gov/kinetics (date of treatment 11.01.2025).
15. Plasma Data Exchange Project [Online]. Available: https://nl.lxcat.net (date of treatment 11.01.2025)
16. N.I. Boyko, A.V. Makogon. High voltage plant with a 3 MW pulse power for disinfection flow of water by nanosecond discharges in gas bubbles // *Tekhnichna Elektrodynamika*. 2020, № 5, p. 80-83. https://doi.org/10.15407/techned2020.05.080
17. A. Brisset, T. Guenin, P. Tardiveau, A. Sobota. Electron density and temperature in a diffuse nanosecond pulse discharge in air at atmospheric pressure // *Plasma Sources Sci. Technol*. 2023, v. 32, N. 6, p. 065014. DOI 10.1088/1361-6595/acdd96
18. S. Nijdam, J. Teunissen, U. Ebert. The physics of streamer discharge phenomena // *Plasma Sources Science and Technology*. 2020, v. 29, №10, 103001. p. 49. https://doi.org/10.1088/1361-6595/abaa05

Article received 14.04.2025

ЧИСЕЛЬНЕ ДОСЛІДЖЕННЯ ФОРМУВАННЯ НЕГАТИВНОГО СТРИМЕРА ІМПУЛЬСНОГО ВИСОКОВОЛЬТНОГО РОЗРЯДУ В ПОВІТРЯНІЙ БУЛЬЦІ У ВОДІ

М.І. Бойко, А.В. Макогон

Запропонована математична модель формування негативного стримера імпульсного високовольтного розряду в повітряній бульці у воді. Розрахунковим шляхом продемонстровано просторово-часовий розподіл стримера в повітряній бульці, рух стримерної хвилі до границі «газ (плазма)–вода», розтікання розряду по поверхні води, утворення найбільш іонізованої субміліметрової області із концентрацією електронів $\sim 7.2 \cdot 10^{16}$ см$^{-3}$ безпосередньо біля вістря, тоді як у стримерному каналі середня концентрація електронів становить $\sim 3 \cdot 10^{15}$ см$^{-3}$.